Journal of ELECTRONIC MATERIALS, Vol. 46, No. 8, 2017
DOI: 10.1007/s11664-017-5425-9
© 2017 The Minerals, Metals & Materials Society

CrossMark

First-Principles Calculations of Structural, Electronic and Optical Properties of Ternary Semiconductor Alloys ZAs_xSb_{1-x} (Z = B, Al, Ga, In)

S. BOUNAB,[1,2,3,6] A. BENTABET,[3] Y. BOUHADDA,[4] GH. BELGOUMRI,[3] and N. FENINECHE[5]

1.—Physics Department, University of Bejaia, 6000 Bejaïa, Algeria. 2.—Physics Department, University of M'sila, 28000 M'sila, Algeria. 3.—Laboratoire de Caractérisation et Valorisation des Ressources Naturelles (LCVRN), Université de Bordj Bou-Arreridj, 34000 Bordj Bou Arreridj, Algeria. 4.—Unité de Recherche Appliquée en Energies Renouvelables, URAER, Centre de Développement des Energies Renouvelables, CDER, 47133 Ghardaïa, Algeria. 5.—IRTES-LERMPS/FC LAB, UTBM University, Belfort, France. 6.—e-mail: sabrinabounab1@yahoo.fr

We have investigated the structural and electronic properties of the $\boldsymbol{BAs_xSb_{1-x}}$, $\boldsymbol{AlAs_xSb_{1-x}}$, $\boldsymbol{GaAs_xSb_{1-x}}$ and $\boldsymbol{InAs_xSb_{1-x}}$ semiconductor alloys using first-principles calculations under the virtual crystal approximation within both the density functional perturbation theory and the pseudopotential approach. In addition the optical properties have been calculated by using empirical methods. The ground state properties such as lattice constants, both bulk modulus and derivative of bulk modulus, energy gap, refractive index and optical dielectric constant have been calculated and discussed. The obtained results are in reasonable agreement with numerous experimental and theoretical data. The compositional dependence of the lattice constant, bulk modulus, energy gap and effective mass of electrons for ternary alloys show deviations from Vegard's law where our results are in agreement with the available data in the literature.

Key words: Semiconductor alloys ZAs_xSb_{1-x}, *ab initio* calculation, the density functional theory

INTRODUCTION

During the last fifty years, there has been considerable interest in III–V zinc blende semiconductors compounds, because they show mechanical, thermal and electrical promising properties,[1] among them the III-Antimonides (BSb, AlSb, GaSb, and InSb). They have been shown to be an important technological factor in high temperature electronic and optical devices.[1,2] Moreover, the III-Arsenide's (BAs, AlAs GaAs, and InAs) have also considerable use in the manufacture of electric devices.[3] However, some optical devices must have specific properties, which cannot be found in the above compounds. Therefore, the combination of two materials (such as III-Antimonides and III-Arsenides) with different physical properties gives rise to new materials with intermediate properties.[4] In the present work, we have given the importance of the study of the structural, electronic and optical properties of the ternary alloys ZAs_xSb_{1-x} (where $Z = \mathrm{B, Al, Ga,}$ and In). The BAs_xSb_{1-x} alloys reveal considerable importance for the reason that they suggest a new class of materials and open new practical perspectives for band-gap engineering in III–V related materials.[5] The $AlAs_xSb_{1-x}$ is considered as a variable large-gap barrier III–V semiconductor with its properties matched to InP, InAs, or GaSb substrates.[2,6–8] In the other hand, the band-gap of $GaAs_xSb_{1-x}$, makes it an attractive material, which can be used in devices operating at the wave lengths between 1.3 mm and 1.6 mm, such as light-emitting diodes and photodetectors.[8] Among all III–V semiconductors alloys, the $InAs_xSb_{1-x}$ has the lowest band-gap with values that

(Received September 24, 2016; accepted February 28, 2017; published online March 16, 2017)

Table I. Calculated equilibrium zinc-blende lattice constants *a*, bulk modulus *B*, first-order pressure derivative of bulk modulus *B′*, and gap energy E_g for the binary compounds with experimental data also shown for comparison

	a (Å)		*B* (GPa)		*B′*		E_g (eV)		
Compounds	Cal.	Exp.	Cal.	Exp.	Cal.	Exp.	Cal.	Exp.	Other works
BAs	4.72	4.777[a]	144.46	–	4.03	–	1.34	1.45[a] 1.46[g]	1.48[i]
BSb	5.18	–	109.37	–	4.26	–	0.77	–	0.527[h]
AlAs	5.61	5.661[b]	74.3	78.1[b]	4.21	–	1.33	2.17[b]	2.202[j]
AlSb	6.09	6.135[c]	55.56	55.1[d]	4.37	–	1.14	1.696[c]	1.836[j]
GaAs	5.53	5.653[b]	75.16	75.5[b]	4.51	–	1.00	1.424[b]	1.226[j]
GaSb	5.98	6.096[b]	56.44	56.1[b]	4.66	–	0.55	0.75[f] 0.726[b]	0.503[j]
InAs	5.92	5.97[e]	61.41	–	4.59	–	0.20	0.35[k]	0.323[j]
InSb	6.32	6.478[f]	47.37	46[f]	4.70	–	0.22	0.2[c], 0.2352[f]	0.052[j]

[a]Ref. 37.[b]Ref. 14.[c]Ref. 2.[d]Ref. 12.[e]Ref. 13.[f]Ref. 38.[g]Ref. 39.[h]Ref. 40.[i]Ref. 41.[j]Ref. 42.[k]Ref. 43.

can be <0.1 eV at room temperature.[2] Consequently, it may offer the possibility of employing it in the long wavelength optoelectronic devices like lasers[2,9] and photo-detectors.[2,10] This work has the goal to investigate the structural, electronic and optical properties of the IIIAs$_x$Sb$_{1-x}$ alloys based on first-principles pseudopotential calculations; within the virtual crystal approximation (VCA). Thus, in the "Computational Method" section we briefly explain the method of computation. In the "Results and Discussions" section we present our results compared with other theoretical calculations and experimental data. Finally, in the "Conclusion" section, we conclude our work.

COMPUTATIONAL METHOD

Our calculations were performed using the Abinit code based on the density functional theory (DFT)[11] within the local density approximation (LDA). The exchange-correlation potential in the Ceperley–Alder form[15] as parameterized by Perdew and Zunger[16] was used. The interactions between electrons and ions were described using nonlocal, norm-conserving pseudopotentials which were generated using the Hartwigsen–Goedecker–Hutter scheme.[17] The energy cut off of the plane wave basis was chosen as 80 Ha. The special points sampling integration over the Brillouin zone was employed with 8 × 8 × 8 by using the Monkhorst–Pack method.[11] For the alloy system in question, we have used the virtual crystal approximation (VCA),[18] in which the virtual pseudo- potential of the alloy $Z\mathrm{As}_x\mathrm{Sb}_{1-x}$ ($Z =$ B, Al, Ga and In) was constructed by the combination of the pseudo- potential of binary compounds ZAs and ZSb according to Vegard's law:

$$V_{VCA} = xV_{ZAs} + (1-x)V_{ZSb}. \quad (1)$$

We have used the VCA instead of the special quasi-random structure (SQS)[19] to avoid a large

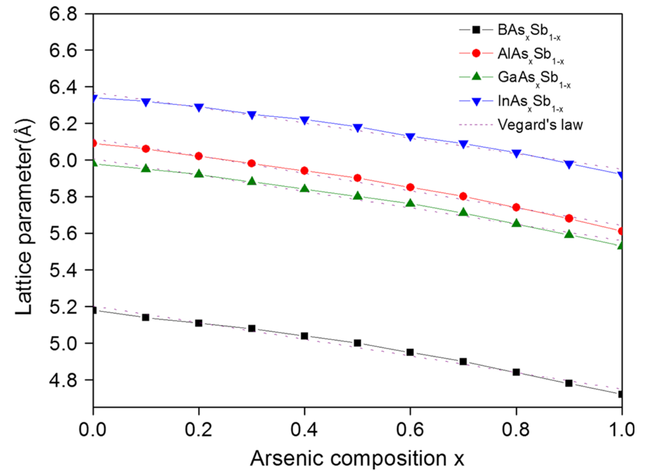

Fig. 1. Composition dependence of the calculated lattice constant for the ternary alloys. BAs$_x$Sb$_{1-x}$, AlAs$_x$Sb$_{1-x}$, GaAs$_x$Sb$_{1-x}$ and InAs$_x$Sb$_{1-x}$. Solid line is the quadratic fit to our data and the dashed line represents Vegard's law.

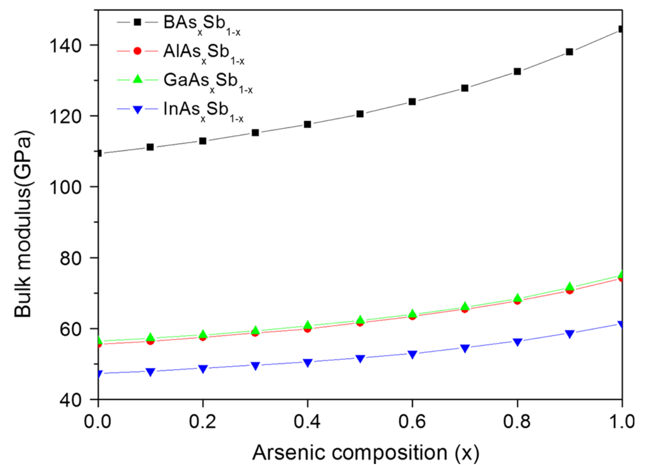

Fig. 2. Composition dependence of the calculated bulk modulus for the ternary alloys. BAs$_x$Sb$_{1-x}$, AlAs$_x$Sb$_{1-x}$, GaAs$_x$Sb$_{1-x}$ and InAs$_x$Sb$_{1-x}$.

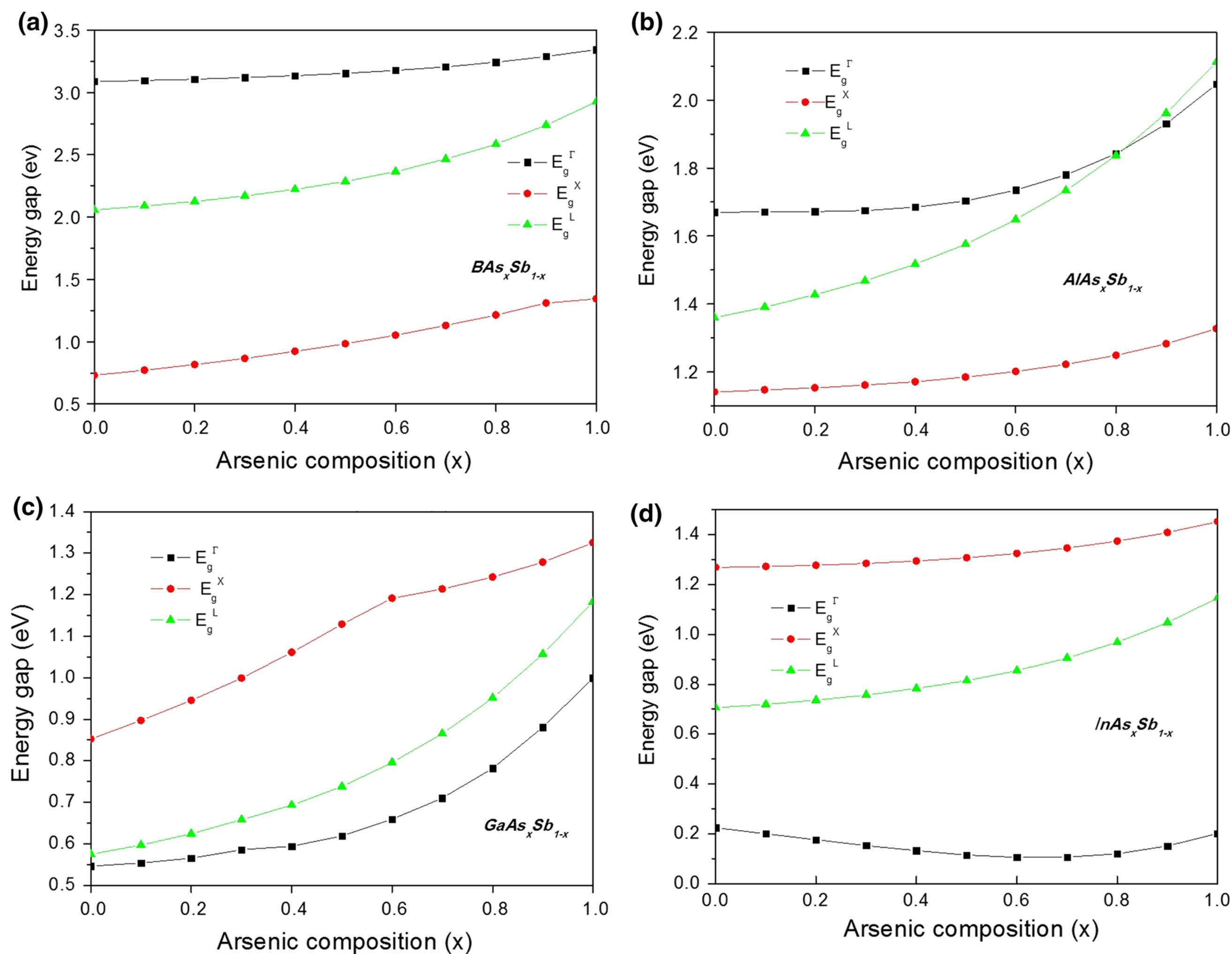

Fig. 3. Energy band gap as a function of arsenic composition for the ternary (a) BAs_xSb_{1-x}, (b) $AlAs_xSb_{1-x}$, (c) $GaAs_xSb_{1-x}$ and (d) $InAs_xSb_{1-x}$.

supercell (needed in SQS), and; therefore, we can reduce the computational time.

RESULTS AND DISCUSSION

In order to study the structural and electronic properties of the alloys in question, we start our calculations with a preliminary study of the zinc-blend binary compounds constituting these alloys Z–As(/Sb) with Z = B, Al, Ga and In (with two atomic positions Z (0,0,0) and As/Sb (1/4,1/4,1/4)). To obtain the structural parameters such as the equilibrium lattice parameter a_0, bulk modulus B and its first pressure derivative B', the total energies versus different volumes around equilibrium, using LDA scheme, are calculated and fitted to the Murnaghan's equation-of-state[20] and are listed in Table I. The gap energy is also presented in Table I compared with theoretical and experimental data.

As can be seen from Table I, our calculated lattice constants and bulk modulus for the binary compounds (III-As and III-Sb) are in good agreement with the experimental values. The computed band structures of binary compounds show a direct band gap ($\Gamma - \Gamma$) for GaAs, GaSb, InAs and InSb, and an indirect band gap ($\Gamma - X$) for BAs, BSb, AlAs and AlSb. As expected, our calculated gap energy of the III–As(/Sb) binary compounds, are underestimated using DFT (usually DFT+LDA underestimated the gap energy by up to 40% for insulator and semiconductors). This is explained in the literature in terms of the effects of self-interaction[15] and particularly of the derivative discontinuity[21–23] of the exchange correlation energy. However, for InSb the gap energy for is underestimated only by 6.9% from the experimental data (see Table I). This is due to the fact that In and Sb have close electronic configurations (correlated 4d electrons) which make the systematic error in the description and in the construction of the pseudo-potential and the exchange-correlation for the two atoms (In and Sb), smaller compared to very different electronic configurations for the other compounds.

For the alloy system, we have used the virtual crystal approximation (VCA). Figure 1 displays the

Table II. The optical band gap bowing for BAs_xSb_{1-x}, $AlAs_xSb_{1-x}$, $GaAs_xSb_{1-x}$ and $InAs_xSb_{1-x}$ alloys compared with other predictions (all values are in eV)

	b					
	Present work			**Other works**		
	Γ	***X***	***L***	***Γ***	***X***	***L***
BAs_xSb_{1-x}	0.25	0.23	0.82	–	0.178[a] 0.109[a]	–
$AlAs_xSb_{1-x}$	0.62	0.20	0.64	0.724[b] 0.691^{c}_{exp}	0.322[b] 0.25^{c}_{exp}	0.489[b] 0.474^{c}_{exp}
$GaAs_xSb_{1-x}$	0.61	−0.15	0.56	1.371[b] 1.2^{c}_{exp}	0.481[b], 0.31^{c}_{exp}	0.362[b] 0.248^{c}_{exp}
$InAs_xSb_{1-x}$	0.39	0.21	0.45	0.728[d]	–	–

[a]Ref. 27.[b]Ref. 8.[c]Ref. 26.[d]Ref. 3.

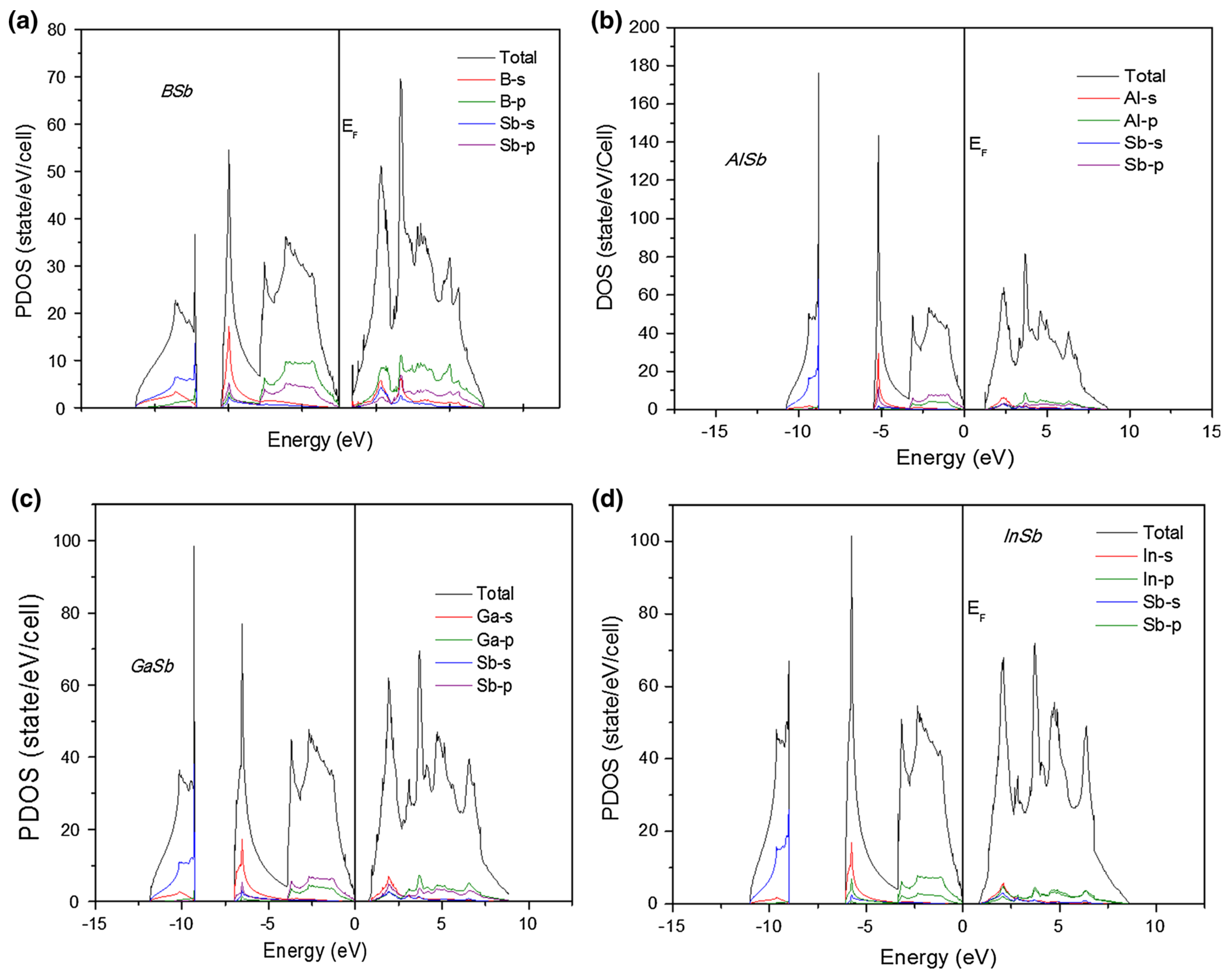

Fig. 4. The electronic partial density of states (PDOS) as a function of the energy for the binary (a) BSb, (b) AlSb, (c) GaSb and (d) InSb. The Fermi level is set to zero energy.

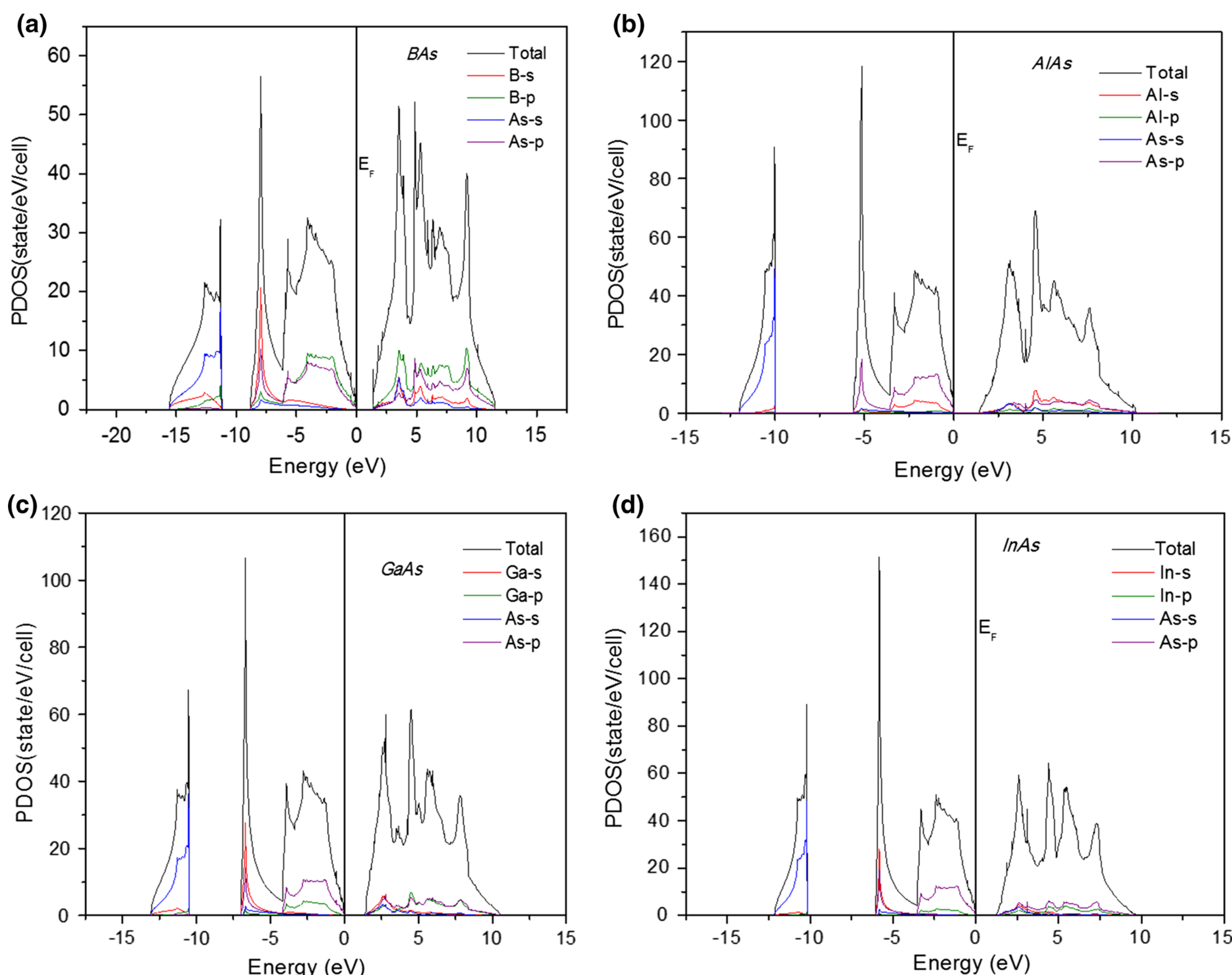

Fig. 5. The electronic partial density of states (PDOS) as a function of the energy for the binary (a) BAs, (b) AlAs, (c) GaAs and (d) InAs. The Fermi level is set to zero energy.

evolution of the calculated equilibrium lattice parameter as a function of the As concentration for BAs_xSb_{1-x}, $AlAs_xSb_{1-x}$, $GaAs_xSb_{1-x}$ and $InAs_xSb_{1-x}$ alloys. Our results, obtained by fitting the calculated values with a polynomial function, shows a slight deviation from Vegard's law for all of the four alloys, with small upward bowing parameters equal to −0.200 Å and −0.188 Å for the BAs_xSb_{1-x} and $AlAs_xSb_{1-x}$, respectively, and −0.189 Å for $GaAs_xSb_{1-x}$ and $InAs_xSb_{1-x}$ alloys. The deviation from Vegard's law for all of the four compounds is caused by the large mismatches of the lattice constants of binary semiconductors. For example, BAs_xBs_{1-x}: BAs and BSb have different lattice constants 4.72 Å and 5.18 Å, respectively.

Figure 2 displays the variation of the bulk modulus versus arsenic concentrations. Our results show positive bowing parameters with 25.66, 13.08 (The.[8]:10.1 GPa),14.19 (The.:8.4 GPa[8]; Exp.:19 GPa[24]) and 10.63 GPa, for the BAs_xSb_{1-x}, $AlAs_xSb_{1-x}$, $GaAs_xSb_{1-x}$ and $InAs_xSb_{1-x}$, respectively. The large bowing value for BAs_xSb_{1-x} compared to those for $AlAs_xSb_{1-x}$, $GaAs_xSb_{1-x}$ and $InAs_xSb_{1-x}$ is due to the considerable mismatch of the bulk modulus of BAs and BSb compounds.

In Fig. 3, we report the evolution of the direct and indirect band gap energies (E_g^{Γ}, E_g^{X} and E_g^{L}) versus arsenic concentration for the ZAs_xSb_{1-x} alloys (with $Z = B, Al, Ga$ and In) in zinc blende structure. As one can see, all studied band gap energies increase non-linearly with increase of the arsenic concentration. Indeed, we can see also that the BAs_xSb_{1-x} and $AlAs_xSb_{1-x}$ alloys are indirect gap materials, whereas the $GaAs_xSb_{1-x}$ and $InAs_xSb_{1-x}$ are direct-gap materials.

The bowing parameter b is an important quantity for investigating the band gap energy ternary alloys.[25] This parameter can be derived directly

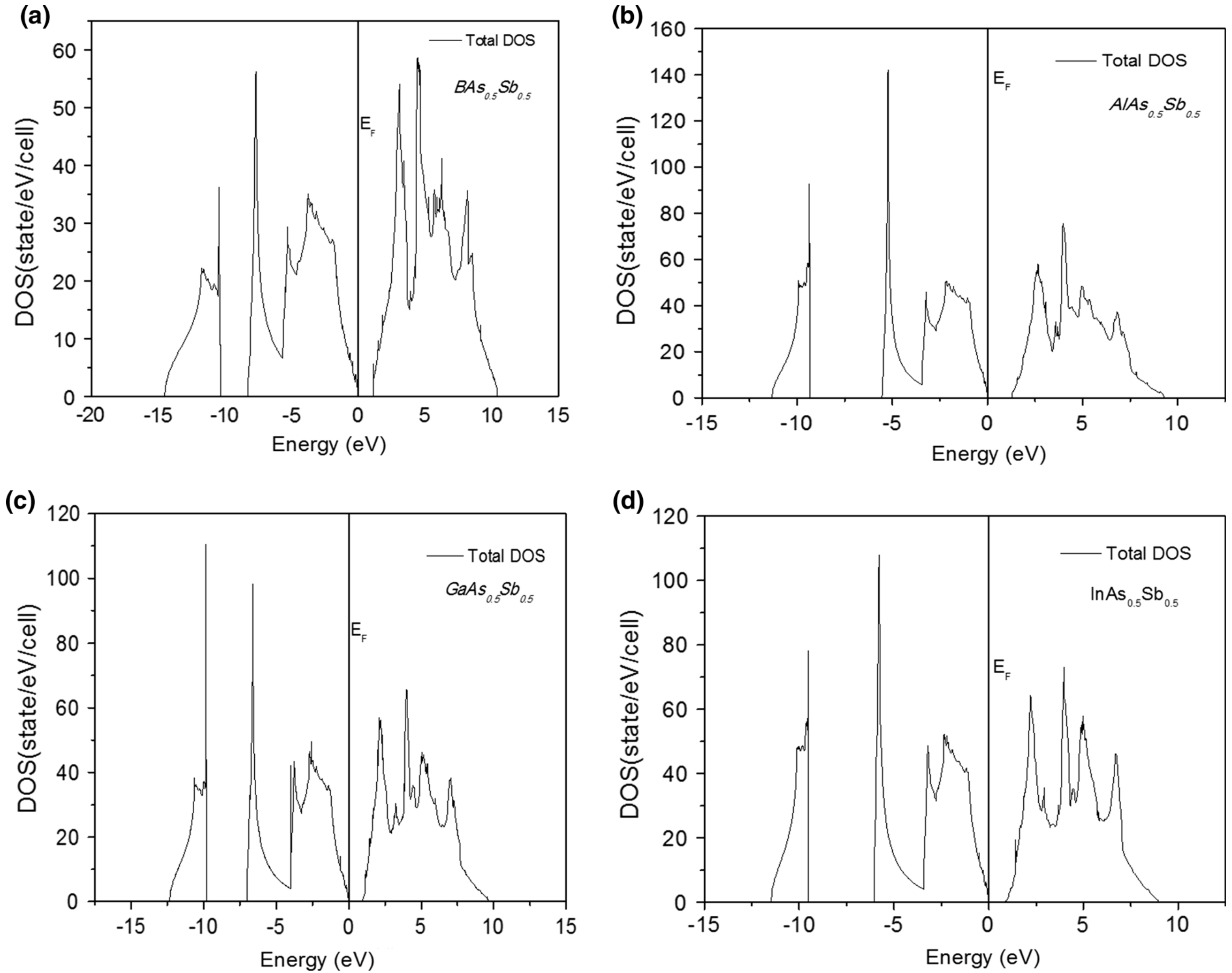

Fig. 6. The electronic density of states (DOS) as a function of the energy for (a) $BSb_{0.5}As_{0.5}$, (b) $AlSb_{0.5}As_{0.5}$, (c) $GaSb_{0.5}As_{0.5}$ and (d) $InSb_{0.5}As_{0.5}$ ternary alloys. The Fermi level is set to zero energy.

from the parabolic term of the second-order empirical relation of the ternary alloy energy band gap:

$$E_g(x) = xE_g^{ZAs} + (1-x)E_g^{ZSb} - bx(1-x), \qquad (2)$$

where E_g^{ZAs} and E_g^{ZSb} are the energy band gaps of ZAs and ZSb (with $Z = \mathrm{B, Al, Ga}$ and In) binary compounds, respectively. So, we note that a positive value of b represents a downward bowing (parabolic term), otherwise an upward bowing if b is negative. Our calculations, obtained by a quadratic fit of the calculated band gaps as a function of the As concentration for alloys of interest, are presented with some available theoretical and experimental values in Table II. In view of Table II, we note that our obtained values of the optical band gap bowing, downward, for the four studied ternary alloys are relatively in disagreement with those reported both experimentally [26, Reference in 3] and theoretically,[8,27] except for the $AlAs_xSb_{1-x}$ alloys, from which we can observe that the band gap bowing parameters of this alloys are in reasonable agreement ($b^L = 0.64$ Exp.[26]: 0.474; $b^\Gamma = 0.62$ Exp.[26]: 0.691 and $b^X = 0.20$ Exp.[26]: 0.25 eV). Therefore, we can explain this difference in bowing as due to the disorder effect, which is not taken into account by the VCA. It may also be noted that the materials with direct gaps (the $GaAs_xSb_{1-x}$ and $InAs_xSb_{1-x}$ with bowing parameters equal 0.61 eV and 0.39 eV respectively) are more affected by the compositional disorder compared to the materials with indirect gap (the BAs_xSb_{1-x} and $AlAs_xSb_{1-x}$ with bowing parameters equal to 0.23 eV and 0.20 eV, respectively).

For more details of the electronic proprieties for the four alloys, we calculate the total and partial DOS by means of the tetrahedral method[28] for these materials. In Figs. 4, 5, and 6, we present the partial DOS of binary compounds ($x = 0$ and $x = 1$) and the total densities of states for x = 0.5 for the BAs_xSb_x, $AlAs_xSb_x$, $GaAs_xSb_x$ and the $InAs_xSb_x$ alloys, respectively. From the calculated partial

DOS of binary Compounds ZY (where Z = B, Al, Ga and In; Y = As and Sb), we can note the following observations: The valence band is divided into three zones; the first zone is dominated by the anion $Y-s$ states; while the cation $Z-s$ and anion $Y-p$ states dominate the next zone. The third zone, which is located just below the Fermi level E_F, is dominated by cation Z and anion Y p states. The cation states (Z-s and Z-p) incorporated with the anion states Y-p contribute essentially to the conduction band (especially the lower portion). Note also the strong perturbation of the conduction band minima, which is due to the incorporation of Z and Y atoms.

The effective masses of electrons, which are strongly linked with the carrier mobility, are essential material parameters describing most transport properties of both electrons and holes in semiconductors.[29] It can be obtained from the band structure, and exactly, in the vicinity of the conduction band minima. In three dimensions, a theoretical effective mass in general became a tensor with nine components because the electron acceleration is not collinear. However, k-space can be centered to get an idealized simple case where $E(k)$ is a parabola at $k=0$ (high symmetry point Γ) and, therefore, all off-diagonal elements of the tenser are zero, and the effective mass becomes a scalar,[30] according to $E=\frac{\hbar^2 k^2}{2m^*}$, where m^* denotes the effective mass of the electron. In the present study, we adopt a second-order (parabolic) fit to calculate the effective masses of electrons at the conduction-band minima. Table III lists our results compared with the available experimental and theoretical values. As can be seen, we report a good agreement only for GaAs and AlAs with a value of $0.051m_0$ ($0.067{m_0}^2$) and $0.169m_0$ ($0.15{m_0}^2$) respectively, compared with those recommended in Ref. 2 where m_0 stands for the electron mass in free space. However, the disagreement for the rest of the binary compounds is due to the LDA calculations, which underestimate not only the band gap, but also the electron effective masses (the underestimation of the bang gap is known to reduce the electron effective mass). For the ternary alloys our results obey the following expressions:

$$BAs_xSb_{1-x} : 0.412 + 0.555x - 0.696x^2 \quad (3)$$

$$AlAs_xSb_{1-x} : 0.513 - 0.729x + 0.40x^2 \quad (4)$$

$$GaAs_xSb_{1-x} : 0.057 - 0.014x + 0.008x^2 \quad (5)$$

$$InAs_xSb_{1-x} : 0.051 - 0.011x + 0.005x^2 \quad (6)$$

Consequently, the electron effective masses increase non-linearly with increasing of concentration x for BAs_xSb_{1-x} and $AlAs_xSb_{1-x}$ with an upward bowing ($0.696m_0$) and downward bowing parameter ($0.40m_0$) respectively, while for the $GaAs_xSb_{1-x}$ and $InAs_xSb_{1-x}$ are almost linear.

The refractive index and dielectric constants represent important physical parameters that describe their optical properties.[31] Their values are needed for devices such as photonic crystals, waveguides, solar cells and detectors.[32] The concentration dependence of the static refractive indices has been computed using the following empirical methods: the modified Moss-relation suggested by Moss using an atomic model[33] and the relation of Ravindra et al.[34] which determines linearly the variation of refractive index with energy gap in semiconductors, as well as the empirical relation proposed by Hervé and Vandamme[35] All of these relations are directly related to the fundamental energy band gap (E_g) as follows:

1. The Moss formula

$$n^4 E_g = k \quad (7)$$

k is a constant with a value of 95 eV.

2. The Ravindra et al. relation,

$$n = 4.084 - 0.62E_g. \quad (8)$$

3. The Hervé and Vandamme empirical expression,

Table III. The electron effective mass (in units of free electron mass) in BAs_xSb_{1-x}, $AlAs_xSb_{1-x}$, $GaAs_xSb_{1-x}$ and $InAs_xSb_{1-x}$ alloys compared with other predictions

	m_e^*	
x	This work	Other work
BAs_xSb_{1-x}		
0	0.40	0.14[a]
0.3	0.471	–
0.7	0.420	–
1	0.339	–
$AlAs_xSb_{1-x}$		
0	0.544	0.14[b]
0.3	0.304	–
0.7	0.21	–
1	0.169	0.15[b]
$GaAs_xSb_{1-x}$		
0	0.056	0.039[b]
0.3	0.0054	–
0.7	0.051	–
1	0.051	0.067[b]
$InAs_xSb_{1-x}$		
0	0.051	0.0135[b]
0.3	0.049	–
0.7	0.046	–
1	0.046	0.026[b]

[a]Ref. 44. [b]Ref. 2.

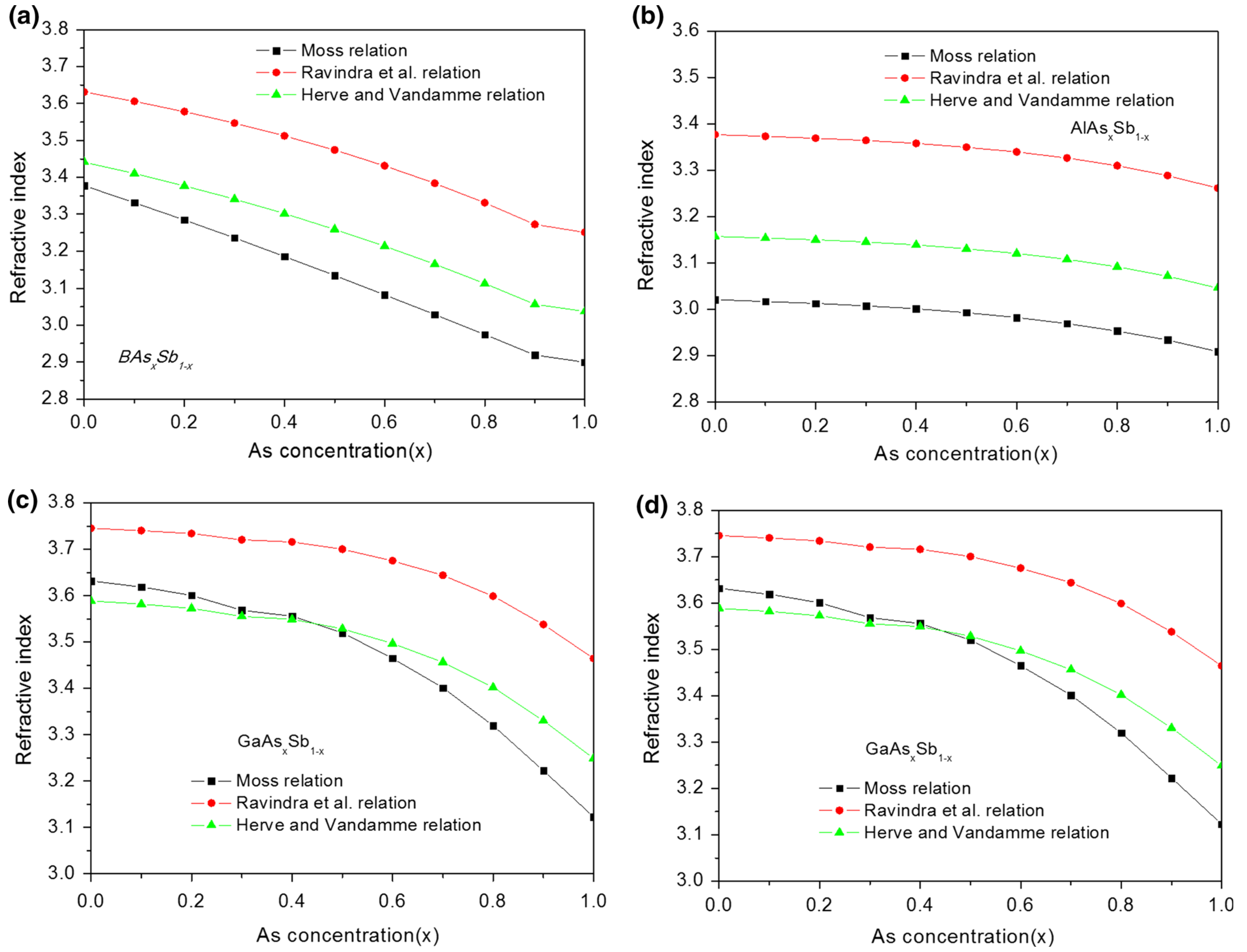

Fig. 7. Refractive index in (a) $BAs_xSb_{1-x}1$, (b) $AlAs_xSb_{1-x}$, (c) $GaAs_xSb_{1-x}$ and (d) $InAs_xSb_{1-x}$ alloys as a function of As concentration (x).

$$n = \sqrt{1 + \left(\frac{13.6}{E_g + 3.4}\right)^2}, \quad (9)$$

where n is the refractive index.

In Fig. 7, we have plotted these relations for refractive index as a function of arsenic concentration of the alloys of interest ($BAs_xSb_{1-x}1$, $AlAs_xSb_{1-x}$, $GaAs_xSb_{1-x}$ and $InAs_xSb_{1-x}$). We observe that for all models used, the refractive index for these alloys decreases with increasing As concentration (x), except the Moss relation for the $InAs_xSb_{1-x}$ alloy, for which one sees an increase with increasing As concentration (x) until $x = 0.6$ followed by a rating decrease up to $x = 1$. This unusual behavior in comparison to the rest of the alloys is another confirmation of the failure of the Moss relation at lower gap energy. Indeed, Herve et al.[35] and Tripathy[36] found that the Moss relation gives a strongest deviation at lower energy gaps (<1.43 eV) as our case of $InAs_xSb_{1-x}$ alloy (0.22–0.20 eV).

The high-frequency dielectric constant (ε_∞) of a material is related to the refractive index as:

$$\varepsilon_\infty = n^2. \quad (10)$$

The obtained results are listed in Table IV. Our calculated results are in close agreement with the available experimental data given in Ref. 36. Furthermore, the composition dependence of (ε_∞) for the $BAs_xSb_{1-x}1$, $AlAs_xSb_{1-x}$, $GaAs_xSb_{1-x}$ and $InAs_xSb_{1-x}$ alloys are displayed in Fig. 8. It can be seen from this figure that except for the Moss relation for the $InAs_xSb_{1-x}$ alloy, which is related to their lower energy gaps, all other relations show a common trend.

Table IV. The high-frequency dielectric constant (ε_∞) of $BAs_xSb_{1-x}1$, $AlAs_xSb_{1-x}$, $GaAs_xSb_{1-x}$ and $InAs_xSb_{1-x}$ alloys for different As concentrations x

Material	Moss relation	The Ravindra et al. relation	Hervé and Vandamme relation	Experimental
BSb	12.163	13.187	11.841	–
$BAs_{0.2}Sb_{0.8}$	11.504	12.803	11.406	–
$BAs_{0.5}Sb_{0.5}$	10.476	12.068	10.623	–
$BAs_{0.8}Sb_{0.2}$	9.432	11.098	9.688	–
BAs	8.967	10.571	9.222	–
AlSb	9.729	11.401	9.97	10.2[a]
$AlAs_{0.2}Sb_{0.8}$	9.678	11.351	9.922	–
$AlAs_{0.5}Sb_{0.5}$	9.549	11.22	9.80	–
$AlAs_{0.8}Sb_{0.2}$	9.299	10.953	9.558	–
AlAs	9.021	10.636	9.278	10.2[a]
GaSb	14.064	14.029	12.878	13.7[a]
$GaAs_{0.2}Sb_{0.8}$	13.826	13.94	12.765	–
$GaAs_{0.5}Sb_{0.5}$	13.209	13.691	12.451	–
$GaAs_{0.8}Sb_{0.2}$	11.752	12.954	11.576	–
GaAs	10.397	12.003	10.558	10.9[a]
InSb	21.972	15.565	15.085	15.7[a]
$InAs_{0.2}Sb_{0.8}$	24.779	15.8	15.465	–
$InAs_{0.5}Sb_{0.5}$	30.739	16.105	15.976	–
$InAs_{0.8}Sb_{0.2}$	30.037	16.078	15.93	–
InAs	23.151	15.674	15.26	12.3[a]

[a]Experimental data cited in Ref. 36.

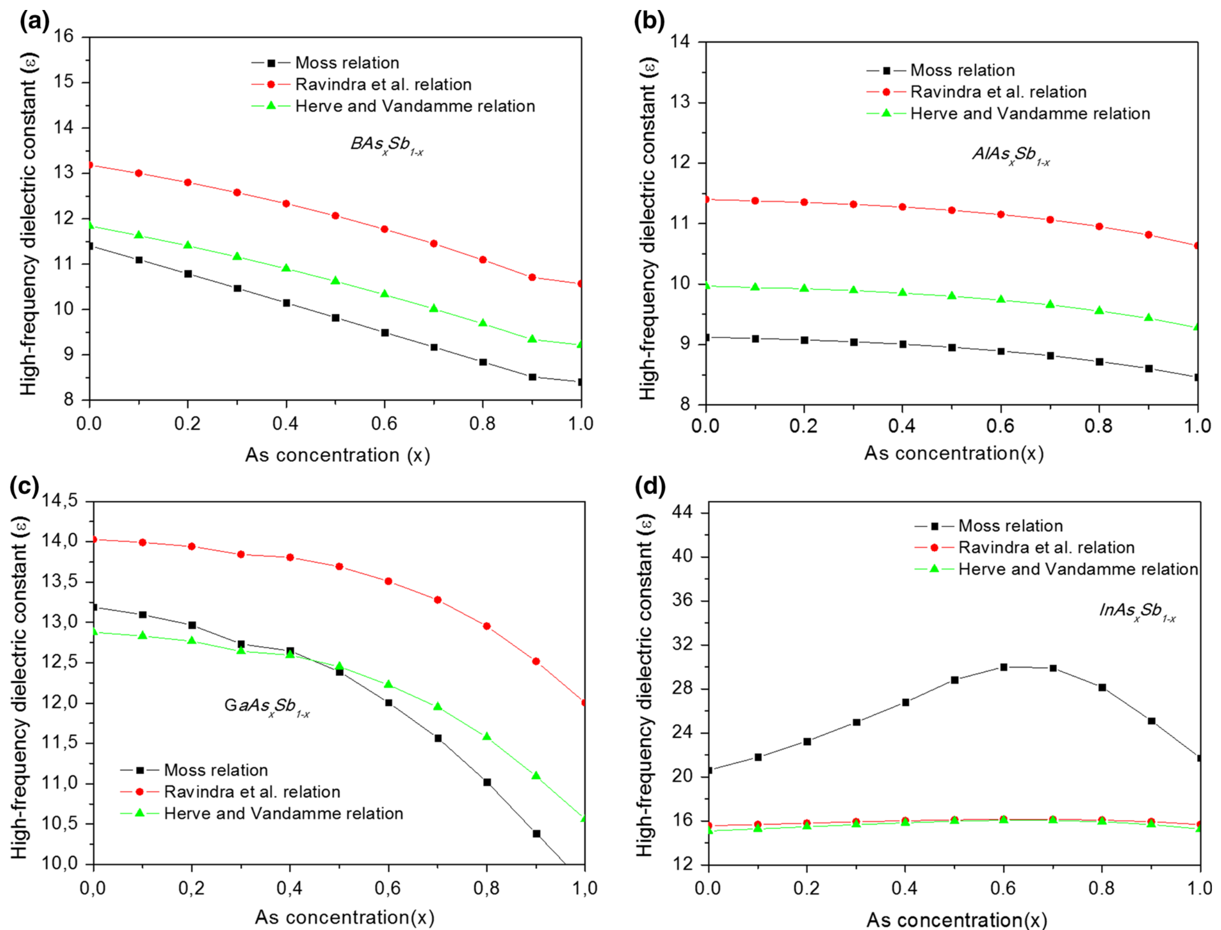

Fig. 8. The high-frequency dielectric constant (ε_∞) of (a) $BAs_xSb_{1-x}1$, (b) $AlAs_xSb_{1-x}$, (c) $GaAs_xSb_{1-x}$ and (d) $InAs_xSb_{1-x}$ alloys as a function of As concentration (x).

CONCLUSIONS

In this paper we have presented a theoretical study of the structural, electronic and optical properties of the BAs_xSb_{1-x}1, $AlAs_xSb_{1-x}$, $GaAs_xSb_{1-x}$ and $InAs_xSb_{1-x}$ alloys in the zinc-blende structure using the first-principles pseudopotential plane-wave method. For the structural properties, our results were found to agree well with the experimental data. We have observed a non-linear behavior of the lattice constant, bulk modulus and band gap with the arsenic concentrations (x) (a relative violation of Vegard's law), which is due to the disorder effect which is not considered by the VCA. the BAs_xSb_{1-x} and $AlAs_xSb_{1-x}$ alloys are indirect gap materials with a downward bowing equal to 0.23 eV and 0.20 eV, respectively, while the $GaAs_xSb_{1-x}$ and $InAs_xSb_{1-x}$ are direct-gap materials with a downward bowing equal to 0.61 eV and 0.39 eV, respectively. Consequently, the latter are more affected by the compositional effect. The electron effective masses for these materials have been calculated, and we find that it increased non-linearly with increase of arsenic concentration for BAs_xSb_{1-x} and $AlAs_xSb_{1-x}$ with an upward bowing ($0.932m_0$) and downward bowing parameter ($0.29m_0$) respectively, while for the $GaAs_xSb_{1-x}$ and $InAs_xSb_{1-x}$ are almost linear. Using empirical methods, it is found that for all used methods the refractive index and the high-frequency dielectric constant (ε_∞) varies non-linearly versus the concentration x. We note also that the Moss relation gives a strongest deviation for the $InAs_xSb_{1-x}$, which is due to the invalidity of this relation for the low energies. For the binary compounds our results are in reasonable agreement with the available data.

Taking into account the few studies on $IIIAs_xSb_{1-x}$ alloys investigated in this work, our results provide predictions and may serve as a support for future investigations.

REFERENCES

1. H. Kalt, *Optical Properties of III–V Semiconductors*, ed. H.-J. Queisser (Berlin: Springer, 1996).
2. I. Vurgaftman, J.R. Meyer, and L.R. Ram-Mohan, *J. Appl. Phys.* 89, 5815 (2001).
3. A. Belabbes, A. Zaoui, and M. Ferhat, *Mater. Sci. Eng. B* 137, 210 (2007).
4. F. El Haj Hassan and H. Akbarzadeh, *Mater. Sci. Eng. B* 121, 171 (2005).
5. B. Bouhafs, H. Aourag, and M. Certier, *J. Phys.: Condens. Matter* 12, 5656 (2000).
6. S. Bhargava, H.-R. Blank, E. Hall, M.A. Chin, H. Kroemer, and V. Narayanamurti, *Appl. Phys. Lett.* 74, 1135 (1999).
7. H.-R. Blank, S. Mathis, E. Hall, S. Bhargava, A. Behres, M. Heuken, H. Kroemer, and V. Narayanamurti, *J. Cryst. Growth* 187, 18 (1998).
8. F. El Haj Hassan, A. Breidi, S. Ghemid, B. Amrani, H. Meradji, and O. Pagès, *J. Alloys Compd.* 499, 80 (2010).
9. P.J.P. Tang, M.J. Pullin, S.J. Chung, C.C. Phillips, R.A. Stradling, A.G. Norman, Y.B. Li, and L. Hart, *Semicond. Sci. Technol.* 10, 1177 (1995).
10. W. Dobbelaere, J. Deboeck, P. Heremans, R. Mertens, G. Borghs, W. Luyten, and J. Van Landuyt, *Appl. Phys. Lett.* 60, 3256 (1992).
11. X. Gonze, J.-M. Beuken, R. Caracas, F. Detraux, M. Fuchs, G.-M. Rignanese, L. Sindic, M. Verstraete, G. Zerah, F. Jollet, M. Torrent, A. Roy, M. Mikami, Ph. Ghosez, J.-Y. Raty, and D.C. Allan, *Comput. Mater. Sci.* 25, 478 (2002).
12. K. Strössner, S. Ves, C.K. Kim, and M. Cardona, *Phys. Rev. B* 33, 4044 (1986).
13. H. Landolt and R. Borstein, *Numerical Data and Functional Relationships in Science and Technology*, ed. O. Madelung and M. Schulz, New Series, Group III, vol. 22 Pt. (Berlin: Springer, 1987).
14. S. Hussain, S. Dalui, R.K. Roy, and A.K. Pal, *J. Phys. D Appl. Phys.* 39, 2053 (2006).
15. D.M. Ceperley and B.J. Alder, *Phys. Rev. Lett.* 45, 566 (1980).
16. J.P. Perdew and A. Zunger, *Phys. Rev. B* 23, 5048 (1981).
17. C. Hartwigsen, S. Goedecker, and J. Hutter, *Phys. Rev. B* 58, 3641 (1998).
18. S. Bounab, Z. Charifi, and N. Bouarissa, *Phys. B* 324, 72 (2002).
19. A. Zunger, S.-H. Wei, L.G. Ferreira, and J.E. Bernard, *Phys. Rev. Lett.* 65, 353 (1990).
20. F.D. Murnaghan, *Proc. Natl. Acad. Sci. USA* 30, 244 (1944).
21. J.P. Perdew, and M. Levy, *Phys. Rev. Lett.* 51, 1884 (1983).
22. L.J. Sham and M. Schlüter, *Phys. Rev. Lett.* 51, 1888 (1983).
23. L.J. Sham and M. Schlüter, *Phys. Rev. B* 32, 3883 (1985).
24. A. Ya, *Handbook Series on Semiconductor Parameters, Ternary and Quaternary III–V Compounds*, ed. M. Levinshtein, S. Rumyantsev, and M. Shur (Singapore: World Scientific, 1999), p. 111.
25. B.T. Liou, S.H. Yen, and Y.K. Kuo, *Proceedings on SPIE 6121* (2006). doi:10.1117/12.644464.
26. O. Madelung, *Semiconductors Basic Data*, 2nd ed. (Berlin: Springer, 1996), pp. 71–172.
27. F. El Haj Hassan. *Phys. Status Solidi B* 242, 3129 (2005).
28. P.E. Blochl, O. Jepsen, and O.K. Anderson, *Phys. Rev. B* 49, 1623 (1994).
29. D.L. Rode, *Semiconductors and Semimetals*, ed. R.K. Willardson and A.C. Beer (New York: Academic Press, 1975), p. 1.
30. Z. Charifi, F. El Haj Hassan, H. Baaziz, Sh. Khosravizadeh, S.J. Hashemifar, and H. Akbarzadeh, *J. Phys.: Condens. Matter* 17, 44 (2005).
31. N.M. Ravindra, P. Ganapathy, and J. Choi, *Infrared Phys. Technol.* 50, 21 (2007).
32. M.A. Ghebouli, B. Ghebouli, A. Bouhemadou, M. Fatmi, and K. Bouamama, *J. Alloys Compd.* 509, 144 (2011).
33. T.S. Moss, *Phys. Status Solidi B* 131, 415 (1985).
34. N.M. Ravindra, S. Auluck, and V.K. Srivastava, *Phys. Status Solidi B* 93, k155 (1979).
35. P.J.L. Herve and L.K.J. Vandamme, *Infrared Phys. Technol.* 35, 609 (1994).
36. S.K. Tripathy, *Opt. Mater.* 46, 244 (2015).
37. T.L. Chu and A.E. Hyslop, *J. Electrochem. Soc.* 121, 412 (1974).
38. O. Madelung, *Semiconductors Basic Data*, 3rd ed. (Berlin: Springer, 2004), pp. 71–172.
39. S.M. Ku, *J. Electrochem. Soc.* 113, 813 (1966).
40. M. Ferhat, B. Bouhafs, A. Zaoui, and H. Aourag, *J. Phys.: Condens. Matter* 10, 7995 (1998).
41. I.H. Nwigboji, Y. Malozovsky, L. Franklin, and D. Bagayoko, *J. Appl. Phys.* 120, 145701 (2016).
42. S. Kacimi, H. Mehnane, and A. Zaoui, *J. Alloys Compd.* 587, 451 (2014).
43. S.E. Stokowski and D.D. Sell, *Phys. Rev. B* 5, 1636 (1972).
44. Y. Yao, D. König, and M. Green, *Sol. Energy Mater. Sol. Cells* 111, 123 (2013).